Int. J. Electrochem. Sci., 8 **(2013)** 10335 - 10349

International Journal of
ELECTROCHEMICAL
SCIENCE
www.electrochemsci.org

Effect of Thiosulfate Ions on the Electrochemical Behavior of Alloy 800

Congwei Fu[1,2], *Jihui Wang*[1,2,*], *Huihui Wang*[2], *Ke Wang*[2]

[1] State Key Laboratory of Hyraulic Engineering Simulation and Safety, Tianjin University, Tianjin 300072, P R China
[2] Tianjin Key Laboratory of Composite and Functional Materials，School of Materials Science and Engineering, Tianjin University, Tianjin 300072, P R China
[*]E-mail: jhwang@tju.edu.cn

Received: 13 May 2013 / *Accepted:* 5 July 2013 / *Published:* 1 August 2013

The effect of thiosulfate ions on the electrochemical behavior of alloy 800 (UNS N08800, ASTM B409) was investigated in simulated neutral steam generator crevice solutions by using electrochemical noise, potentiodynamic polarization and potentiostatic polarization techniques. The results showed that the noise resistance, corrosion potential, breakdown potential and passive range of alloy 800 in the solution containing thiosulfate and chloride ions were lower than that in solution containing thiosulfate or chloride ions alone, whereas the steady state current density of alloy 800 in thiosulfate and chloride containing solution was larger than that in solution containing only thiosulfate or chloride ion. Under the synergistic effect of $S_2O_3^{2-}$ and Cl^- ions, chloride and thiosulfate ions could be successively absorbed into the alloy surface, impeded the passivation of alloy 800 and decreased the corrosion resistance of alloy 800.

Keywords: alloy 800, thiosulfate, chloride, electrochemical behavior, passive film

1. INTRODUCTION

Alloy 800 has a higher resistance to creep and oxidation at elevated temperatures due to its ductile and fully austenitic structure[1], and thus has been extensively used as steam generator (SG) tube materials in the nuclear industries [2-5]. However, degradation of alloy 800 SG tubing could be found merely in tubes at a limited number of stations despite the large number of SG tube operated years accumulated to date. In the SG feedwater, Sulfate is one of the major impurities, which can be reduced to intermediate oxidation state sulfur (IOSS) under the assistance of hydrazine. Among the identified possible IOSS species, thiosulfate ($S_2O_3^{2-}$) is known as one of the reduced sulfur species that

causes corrosion degradation of steel alloys, such as alloy 600, alloy 690 and alloy 800 in chloride containing solution[6-10].

Fang and Staehle [11] investigated the effects of the valence of sulfur on passivation of alloys 600, 690, and 800 at 25°C and 95°C by electrochemical polarization measurements, and found that the decreasing valence of sulfur oxyanions would decrease the stability of passive films of alloys 600, 690, and 800. Increasing the concentration of $S_2O_3^{2-}$ from 10^{-4} mol/L to 1.5 mol/L could significantly increased the passive current density and lowered the breakdown potential. By using linear polarization resistance and mass loss measurements, Ezuber [8] revealed that the presence of thiosulfate seems to activate both anodic and cathodic current densities of steel in chloride solutions. The higher the thiosulfate concentration, the greater the anodic/cathodic current densities were. In Faichuk's work [12], potentiodynamic polarization and electrochemical impedance spectroscopy experiments were conducted to investigate the electrochemical and surface properties of passive film formed on alloy 600 in a thiosulfate solution. Their results showed that the oxide film was composed by a Cr-rich inner layer and a mixed Ni and Fe outer layer, and the composition of outer layer was changed with the applied potential which would result in a change in the impedance behavior. The formation process of oxide film on alloy 600 could be explained by point defect model (PDM). But until now, there is little information about the corrosion behavior of alloy 800 in thiosulfate or thiosulfate- chloride containing solution.

Apart from potentiodynamic polarization, electrochemical impedance spectroscopy and cyclic voltammetry techniques, electrochemical noise method is the only in-situ electrochemical method which does not disturb the corrosion system[13]. Electrochemical noise (EN) is a general term referring to fluctuations in the potential and current generated spontaneously by corrosion processes[14], could characterize the changes in the thermodynamic and kinetic states of metal/solution interface[15]. So EN measurement is becoming one of the most promising methods for detecting corrosion process and exploring the corrosion mechanism [16, 17].

The projective of this paper is to determine the electrochemical behavior of alloy 800 in thiosulfate containing solution by using electrochemical noise, potentiodynamic polarization and potentiostatic polarization techniques, and then the effect of thiosulfate ion on the stability of passive film on alloy 800 could be obtained and understood.

2. EXPERIMENTAL

2.1 Material and simulated solutions

The chemical composition of alloy 800 used is shown in Table 1. The testing sample was cut from alloy 800 tubing with the dimensions of 1.13 mm nominal wall thickness and 15.88 mm outside diameter. And then the samples were connected to a copper wire, embedded into epoxy resin with an exposed area of 0.13 cm^2 and mounted in a PVC holder. Subsequently, the exposed surface was mechanically polished with wet silicon carbide papers in the sequence of 400, 800, 1000, 1500, and 2000 grit, rinsed copiously with deionized water, and then dried in desiccator for 24h.

Three simulated crevice solutions were prepared by using analytical chemical reagents and deionized water, and listed in Table 2.

Table 1. Chemical composition of alloy 800 (wt%)

C	Si	Mn	P	S	Cr	Ni	Co	Ti	Cu	Al	N	Fe
0.017	0.46	0.5	0.012	0.001	21.87	32.78	0.01	0.48	0.02	0.29	0.016	43.2

Table 2. Simulated CANDU SG neutral crevice (NC) chemistry (unit: mol·L^{-1})

Solution	NaCl	KCl	$CaCl_2$	SiO_2	$Na_2S_2O_3$
R1	0	0	0	0	0.075
NC-1	0.30	0.05	0.15	0.05	0
NC-2	0.30	0.05	0.15	0.05	0.075

2.2 Electrochemical noise measurement

All the electrochemical measurements of alloy 800 were carried out in the above R1, NC-1 and NC-2 solutions by using a VersaSTAT 4 electrochemical workstation (Princeton Applied research, USA) and VersaStudio control software.

A three-electrode configuration was used for the electrochemical noise experiment. A saturated calomel electrode (SCE) was used as reference electrode. Two nominally identical electrodes were made by alloy 800, and connected through a zero resistance ammeter (ZRA) mode. By considering the influence of alloy surface condition, one group of electrochemical noise data was collected just after 10 min's immersion of alloy 800 in solution. The other group was recorded from the alloy 800 which was firstly cathodic polarized at -1V (vs. reference electrode) for 10 min to remove all the native oxide. The electrochemical noise test was carried out for a period of 10 hours， with a sampling frequency of 2Hz.

Before the statistical analysis, a 5-order polynomial fitting was applied to remove the direct current (DC) component from original EN data. And the noise resistant R_n was calculated by $R_n=\sigma_E/\sigma_I$, in whichσ_E is the standard deviation of electrochemical potential noise and σ_I is the standard deviation of electrochemical current noise. When both working electrodes have the same activity and the corrosion process is uniform under activation control, the electrochemical noise resistance is inversely proportional to the corrosion rate [17, 18].

According to the shot noise theory for electrochemical noise, the charge in each event q, and the frequency of appearance of these events f_n can be obtained from the voltage and current noise by the equations of $q = \frac{\sqrt{PSD_E}\cdot\sqrt{PSD_I}}{B}$, $f_n = \frac{B^2}{PSD_E \cdot A}$, where PSD_E and PSD_I are the low frequency PSD

values of the potential and current noise respectively, B is the Stern–Geary coefficient and A is the exposed area of electrode[16, 17].

In order to observe the distribution of q and f_n in the corrosion process, paramentes of q and f_n were sorted into ascending order, and then the cumulative probability p was derived as $n/(N + 1)$, where n is the position of the q or f_n value in the sorted list, and N is the total number of values[16].

2.3 Potentiodynamic polarization

The potentiodynamic polarization experiments of alloy 800 in R1, NC-1 and NC-2 solutions were conducted by a using a conventional three-electrode cell with a potential scan rate of 0.1667 mV/s. Alloy 800 with an exposed area of 0.13 cm^2 was used as working electrode, and saturated calomel electrode and Pt were used as reference electrode and counter electrode respectively.

2.4 Potentiostatic polarization

Potentiostatic polarization experiments are always applied to characterize the kinetics of passive film growth and dissolution [19]. The potentiostatic polarization curves of alloy 800 in R1, NC-1 and NC-2 solutions were measured under the selected potentials by using the above conventional three-electrode system. The selected potentials were chosen from the passive range of alloy 800 in the potentiodynamic polarization curves tested in section 2.3. After the tests, the steady state current density, i_{ss} , was obtained at the end of current-time curve.

3. RESULTS

3.1 Electrochemical noise

Fig.1 shows the EN data of alloy 800 without cathodic polarization in R1 solution. It can be seen that with the increasing of immersion time the potential of alloy 800 increases and the current density decreases, which indicates the formation of passive film on alloy 800. About 10000 s later, both the potential and current density tend to fluctuate around a constant value, which suggests that the passive film on alloy 800 reached a steady state.

After removing DC component, EN data of alloy 800 without cathodic polarization in R1 solution under different immersion time are shown in Fig.2. It can be seen that all the potential signals show very high repetition rates of fluctuations with the amplitude lower than 0.6 mV, and the current signals have very low amplitudes. In the early stage of alloy 800 immersed in R1 solution, the fluctuation amplitude of current density is about 300pA·cm^{-2} (Fig.2a). With the increasing of immersion time, the fluctuation amplitude of current density decreases to 125pA·cm^{-2} during the time range of 19200-19250s (Fig.2b), or 150pA·cm^{-2} during the time range of 35000-35050 s (Fig.2c). Similar results could also be observed for alloy 800 in NC-1 and NC-2 solutions. These changes on

electrochemical potential and current signals implied that a passive film was formed on alloy 800 after the immersion in R1, NC-1 and NC-2 solutions.

Fig.3 is the dependence of noise resistance of alloy 800 without cathodic polarization on the immersion time. At the initial stage of immersion, the noise resistance of alloy 800 is almost the same in R1, NC-1 and NC-2 solutions. And then the noise resistance increases with the increasing time of immersion. After 36000s' immersion, the noise resistance of alloy 800 increases to 4.25×10^6 Ω·cm^2 in R1 solution, or 1.40×10^6 Ω·cm^2 in NC-1solution and 1.02×10^6 Ω·cm^2 in NC-2 solution.

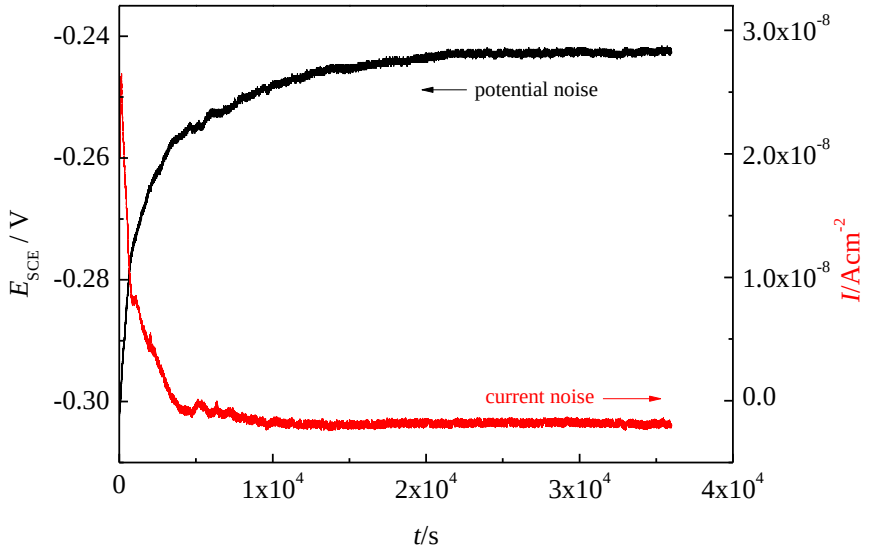

Figure 1. Electrochemical noise data of alloy 800 without cathodic polarization in R1 solution

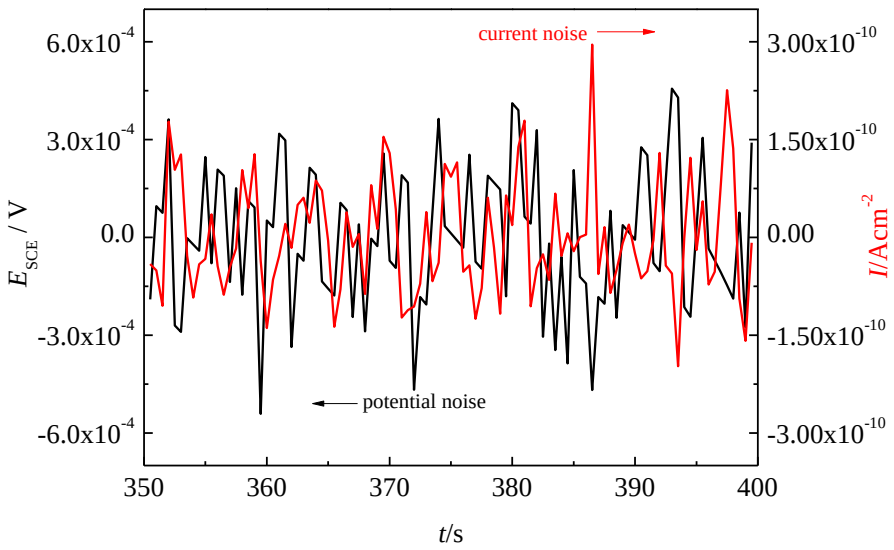

(a)350-400s

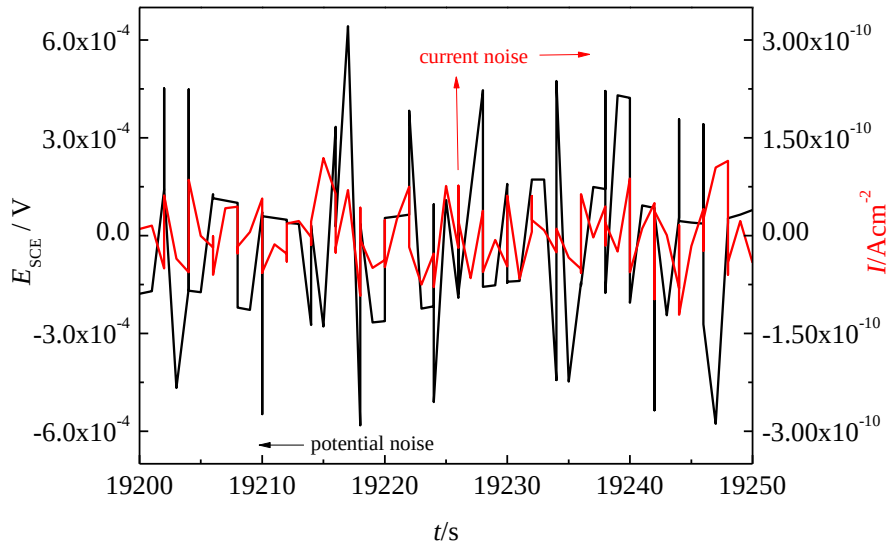

(b) 19200-19250s

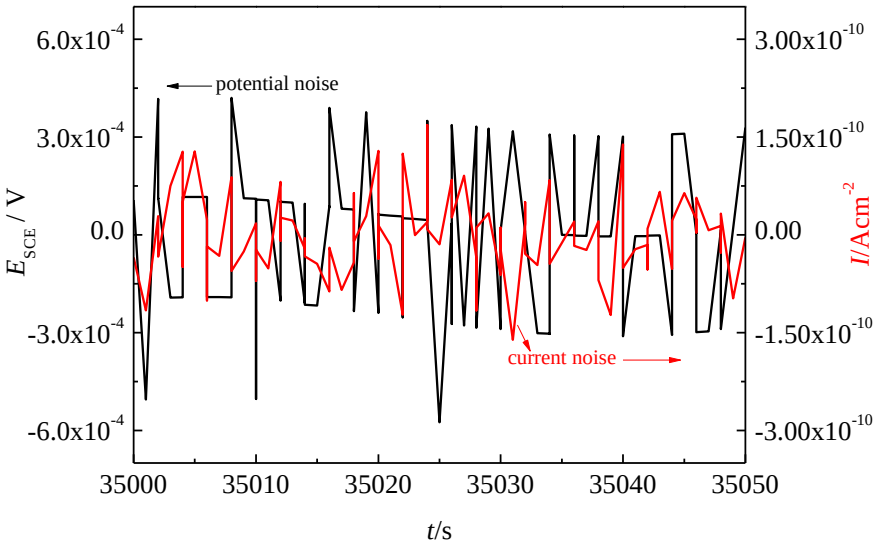

(c) 35000-35050s

Figure 2. Electrochemical noise data (after a dc was removed) of alloy 800 without cathodic polarization in R1 solution under different immersion time, (a)350-400s, (b)19200-19250s, (c)35000-35050s

The cumulative probability of noise resistance for alloy 800 in R1, NC-1 and NC-2 solution is shown in Fig.4. It is observed that the noise resistance of alloy 800 in R1 solution is located between $1.0\times10^6 \sim 5.0\times10^6$ $\Omega\cdot cm^2$, which is the largest among the three solutions. Whereas，the alloy 800 in NC-2 solution has the lowest noise resistance. All these results proves that the noise resistance of alloy 800 in thiosulfate and chloride containing solution is lower than that in the solution containing $S_2O_3^{2-}$

or Cl^- ion alone, i.e. under the synergistic effect of $S_2O_3^{2-}$ and Cl^- ions alloy 800 has a higher corrosion rate, which is similar with the results of [8].

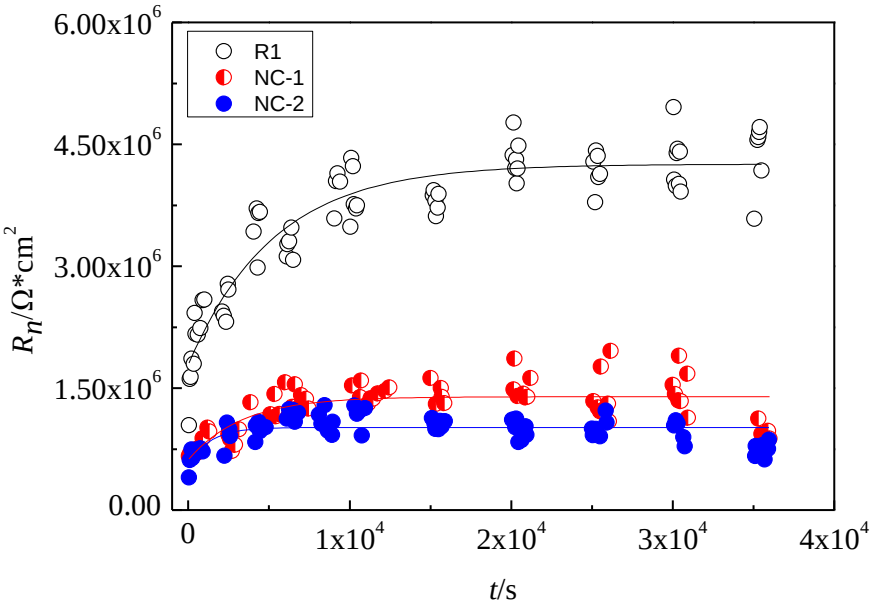

Figure 3. Dependence of noise resistance of alloy 800 without cathodic polarization in R1, NC-1 and NC-2 solution with immersion time.

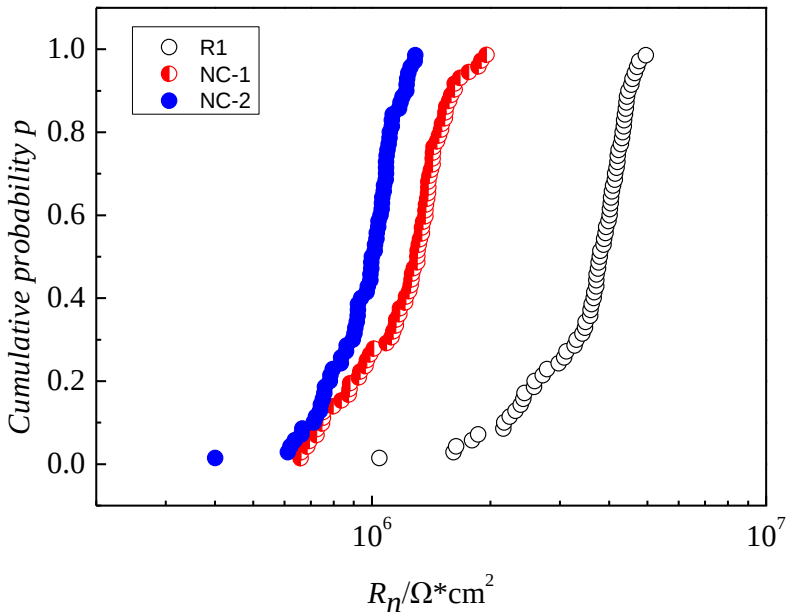

Figure 4. Cumulative probability of noise resistance for alloy 800 without cathodic polarization in R1, NC-1 and NC-2 solution.

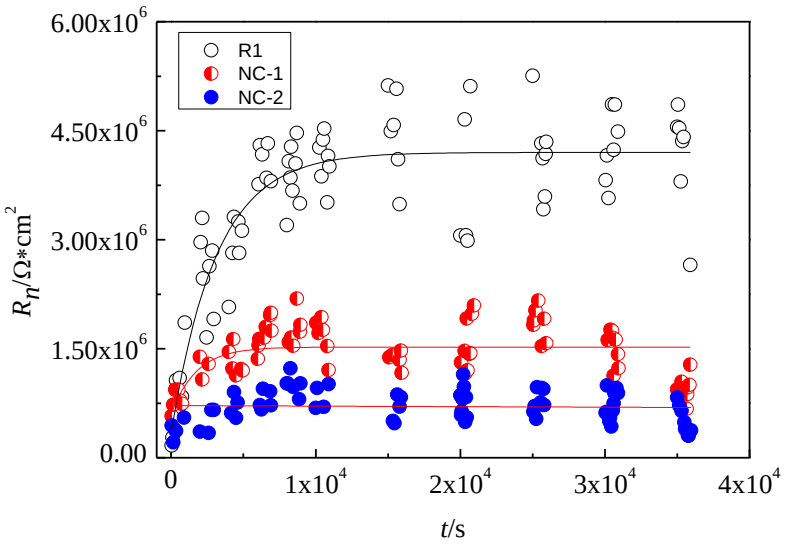

Figure 5. Dependence of noise resistance of alloy 800 with cathodic polarization in R1, NC-1 and NC-2 solution with immersion time.

Fig.5 is the noise resistance of alloy 800 with cathodic polarization in R1, NC-1 and NC-2 solutions. Fig.6 is the cumulative probability of noise resistance for alloy 800 in R1, NC-1 and NC-2 solution. As compared with alloy 800 without cathodic polarization in Fig.3 and Fig.4, the noise resistance of alloy 800 with cathodic polarization in R1, NC-1 and NC-2 solutions has the similar regularity with immersion time and cumulative probability. At the initial stage of immersion, the noise resistance of alloy 800 with cathodic polarization in R1 solution is obviously lower than that without cathodic polarization. But at end of 10 hours' immersion, there is almost no obvious difference in noise resistance of alloy 800 between with and without cathodic polarization. The noise resistance of alloy 800 with cathodic polarization in NC-1 solution after 10 hours' immersion is about 1.50×10^6 $\Omega\cdot cm^2$, which is almost the same with that of alloy 800 without cathodic polarization (Fig.3). But the noise resistance of alloy 800 with cathodic polarization in NC-2 solution after 10hours' immersion (0.69×10^6 $\Omega\cdot cm^2$) is much less than that of alloy 800 without cathodic polarization (1.02×10^6 $\Omega\cdot cm^2$). All these results meant that the cathodic polarization treatment has a little effect on the noise resistance of alloy 800 in $S_2O_3^{2-}$ or Cl^- containing solution, but greatly decrease the noise resistance of alloy 800 in $S_2O_3^{2-}$ and Cl^- containing solution. This phenomenon is probably caused by the combination of the reduction of native oxide film by cathodic polarization and the formability of passive film in $S_2O_3^{2-}$, Cl^- and $S_2O_3^{2-}$-Cl^- containing solution.

Fig.7 and Fig.8 are the cumulative probability of f_n and q for alloy 800 with cathodic polarization in R1, NC-1 and NC-2 solution. From the frequency f_n of electrochemical noise events, no significant differences are found among the R1, NC-1 and NC-2 solutions (Fig.7). But the average charge q in each event is quite different among the three solutions. The average charge distribution of alloy 800 is increased by the order of R1, NC-1 and NC-2 solution under the same cumulative

probability (Fig.8). This implies that the anodic dissolution rate of alloy 800 in $S_2O_3^{2-}$ and Cl^- containing solution is greater than that in $S_2O_3^{2-}$ or Cl^- containing solution.

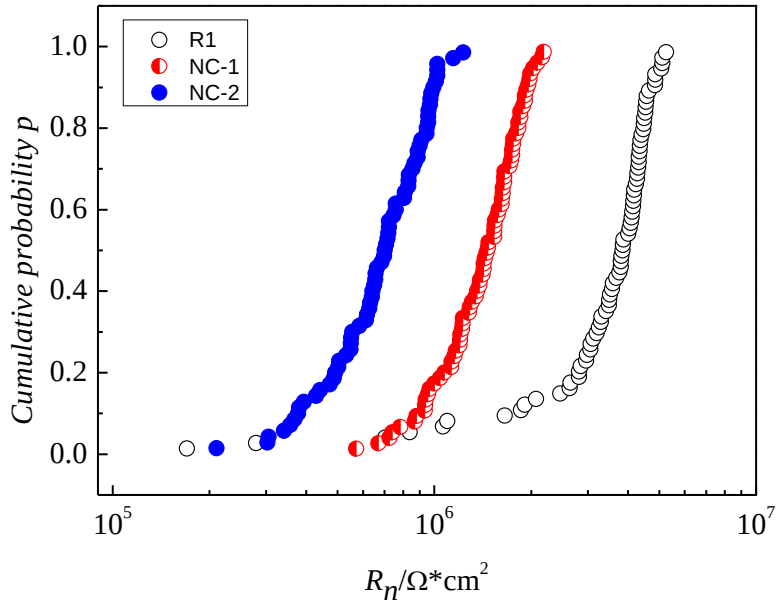

Figure 6. Cumulative probability of noise resistance for alloy 800 with cathodic polarization in R1, NC-1 and NC-2 solution.

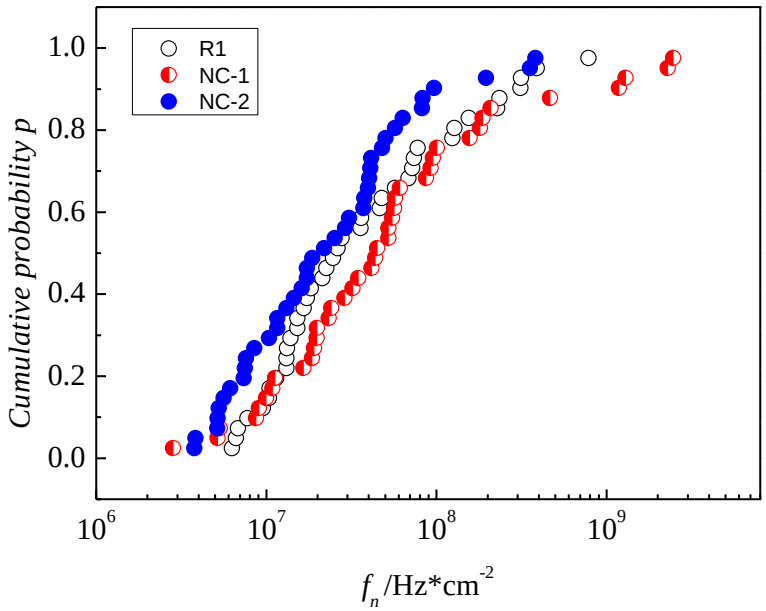

Figure 7. Cumulative probability of f_n for alloy 800 with cathodic polarization in R1, NC-1 and NC-2 solution

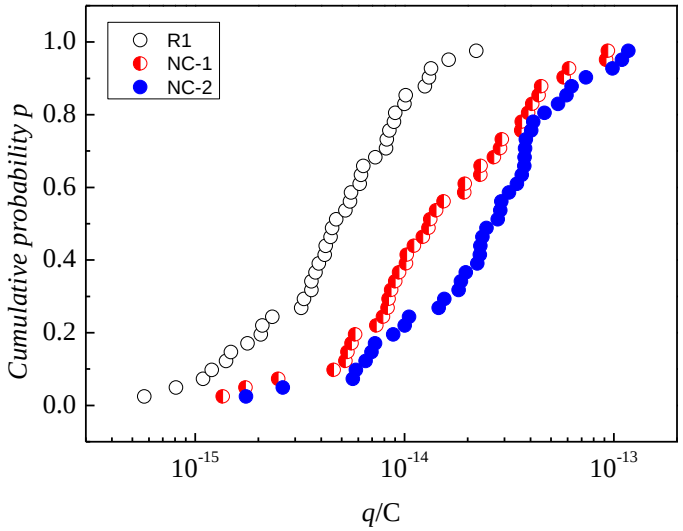

Figure 8. Cumulative probability of *q* for alloy 800 with cathodic polarization in R1, NC-1 and NC-2 solution

3.2 Potentiodynamic polarization

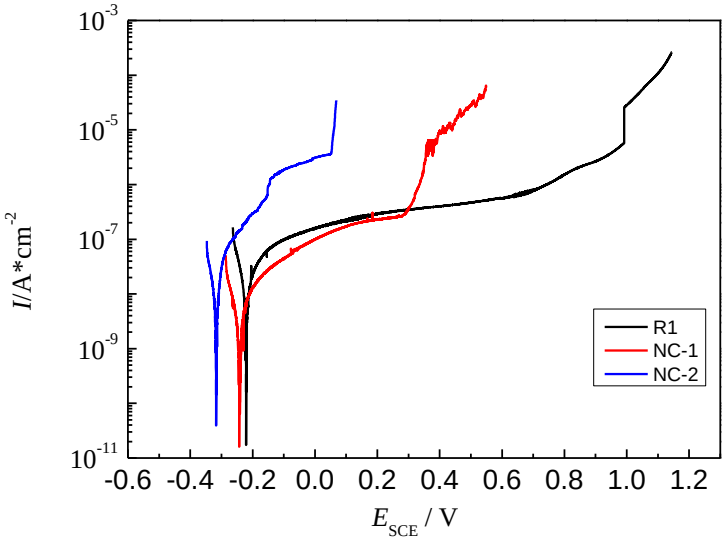

Figure 9. Potentiodynamic polarization curves of alloy 800 in R1, NC-1 and NC-2 solutions

Fig.9 is the potentiodynamic polarization curves of alloy 800 in R1, NC-1 and NC-2 solution, and the corrosion potential, E_{corr}, breakdown potential, E_b, passive range and corrosion current, i_{corr}, of alloy 800 in three solutions are listed in Table 3 and plotted in Fig.10. It is seen that the corrosion potential, breakdown potential and passive range of alloy 800 were decreased by the order R1, NC-1 and NC-2 solution. The corrosion current of alloy 800 in NC-2 is higher than that in R1 and NC-1.

These results also proves that the corrosion resistance of alloy 800 in in $S_2O_3^{2-}$ and Cl^- containing solution is lower than that in $S_2O_3^{2-}$ or Cl^- containing solution. Similar observations have been reported elsewhere for alloy 690[6].

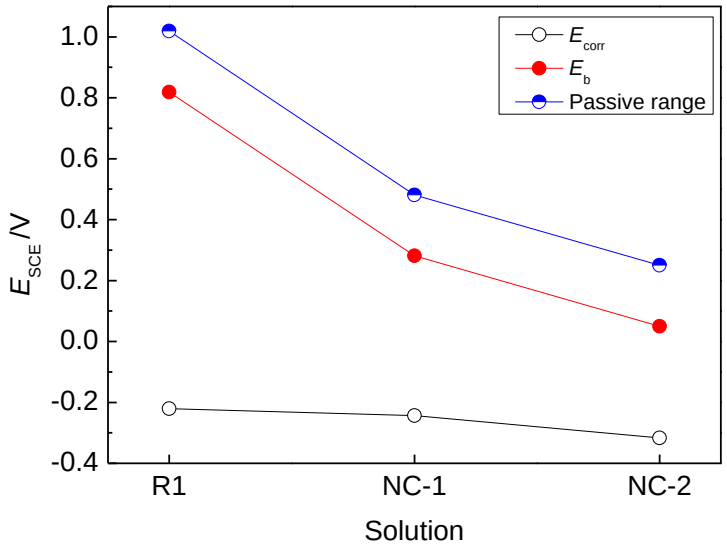

Figure 10. Corrosion potential, breakdown potential and passive range of alloy 800 in R1, NC-1 and NC-2 solution.

Table 3. Corrosion potential and breakdown potential of alloy 800 in R1, NC-1 and NC-2 solution

Solution	E_{corr}/V	E_b/V	Passive range/V	i_{corr} /nA·cm^{-2}
R1	-0.221	0.819	-0.200~0.820	1.948
NC-1	-0.243	0.281	-0.200~0.280	1.400
NC-2	-0.317	0.05	-0.200~0.050	3.126

3.3 Potentiostatic polarization

Fig.11 is the current density-time curves of alloy 800 under potentiostatic polarization in R1, NC-1 and NC-2 solution. The steady state current density of alloy 800 in three solutions is shown in Fig.12. The dependence of the passive current density in the steady state on the formation potential may be related to the change in the structure and properties of the passive film[20, 21]. It can be observed that the steady state current density of alloy 800 increased with the increasing of polarized potential, which indicated that the passive current density was dependent of the formation potential. And the passive current density of alloy 800 in NC-2 solution is higher than that in NC-1 and R1 solution under the same polarized potential. It also meant that the stability of passive film on alloy 800 in in $S_2O_3^{2-}$ and Cl^- containing solution is lower than that in $S_2O_3^{2-}$ or Cl^- containing solution.

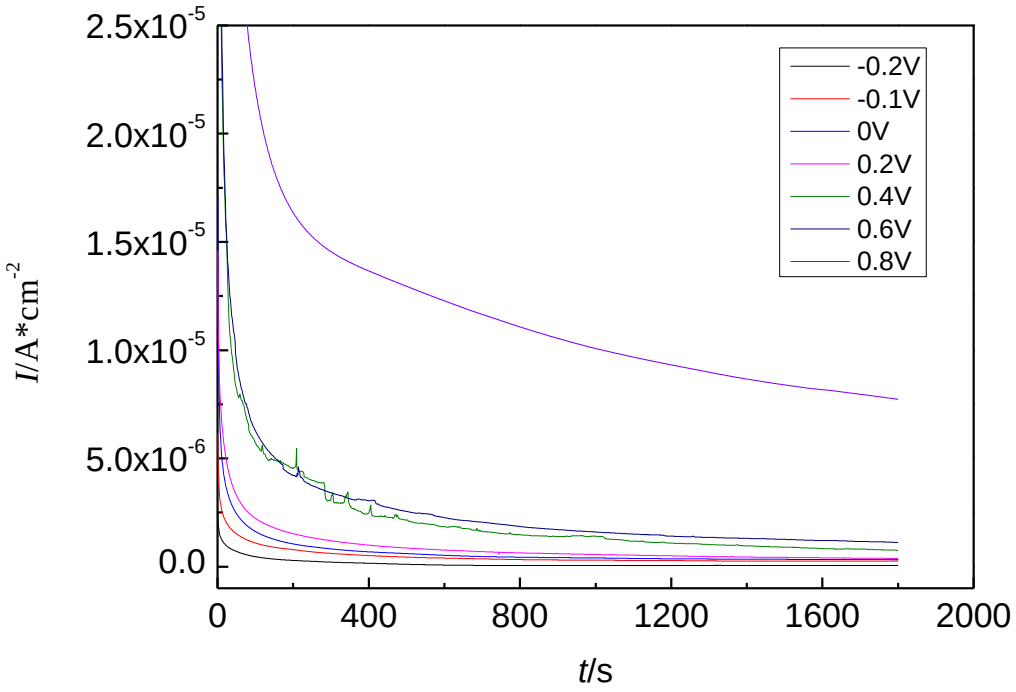

(a) R1 solution

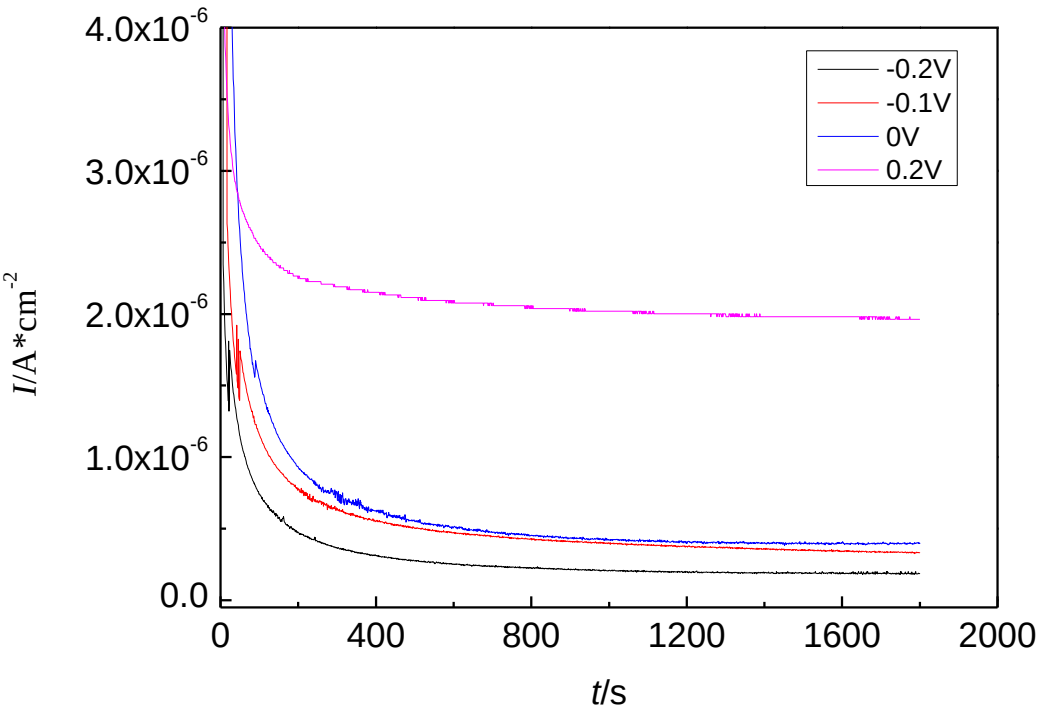

(b) NC-1 solution

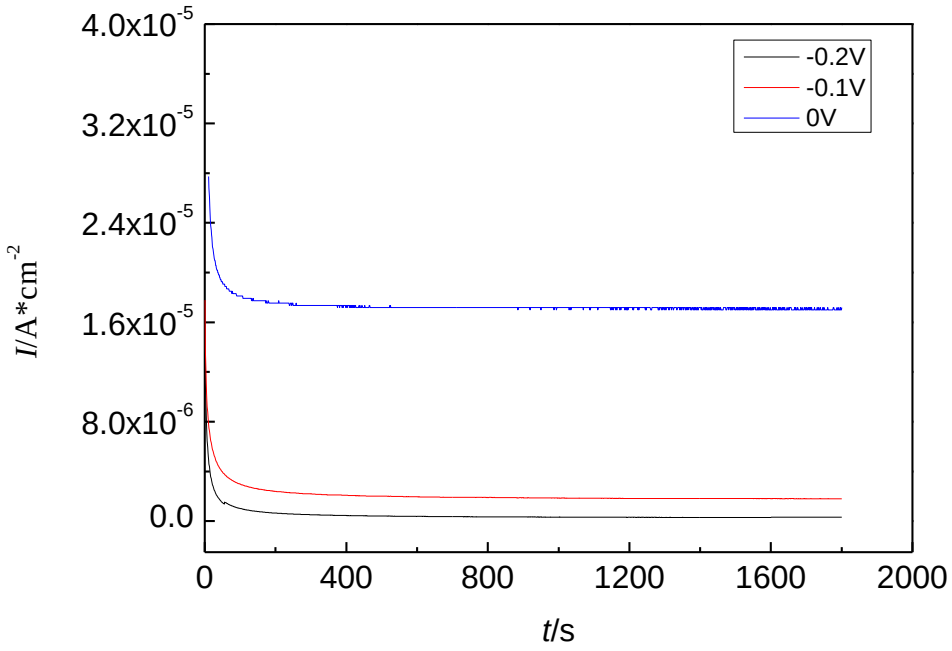

(c) NC-2 solution

Figure 11. Potentiostatic polarization curves of alloy 800 in R1, NC-1 and NC-2 solutions under different polarized potentials

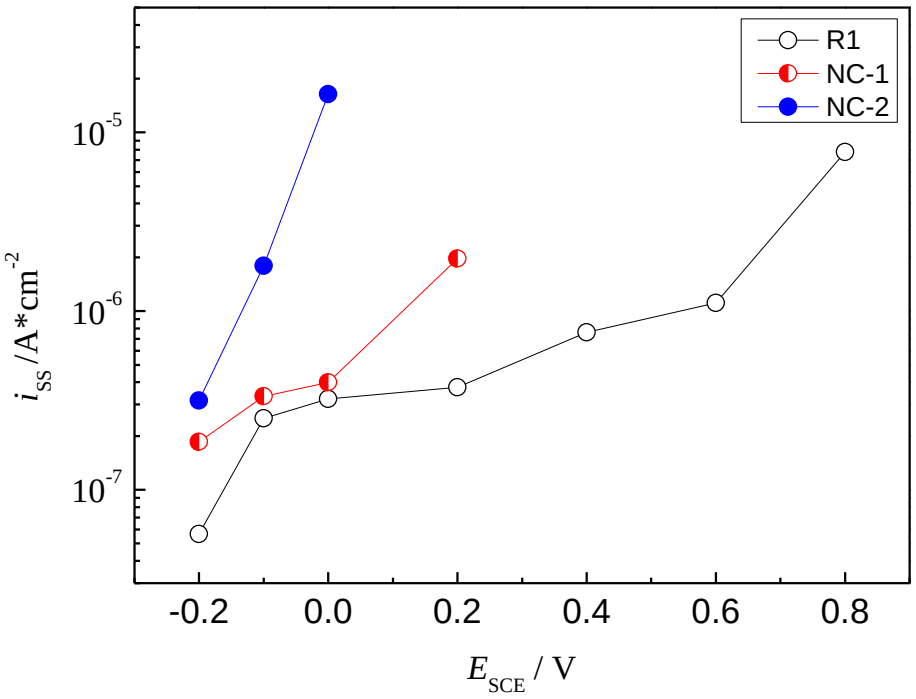

Figure 12. Steady state current density of alloy 800 in R1, NC-1 and NC-2 solutions under different polarized potentials.

4. DISCUSSIONS

From the above results, alloy 800 has a higher corrosion resistance and a better passive stability in film in $S_2O_3^{2-}$ or Cl^- ions containing solution. But in the solution coatining both $S_2O_3^{2-}$ and Cl^- ions (NC-2 solution), the corrosion ressitance and passive film formability were greatly deteriorate.

In the point defect model[22, 23], the chloride ion is absorbed into the oxygen vacancies at the barrier/outer layer interface. The absorption of chloride into the interfacial oxygen vacancy increases the vacancy concentration of local cation, which increases the electromigration-dominated flux of cation vacancies from the barrier layer/outer layer interface to the metal/barrier interface. When arrived at the metal/barrier layer interface, cation vacancies are annihilated by an oxidative injection of cation from the metal into the film. However, if the rate of annihilation cannot accommodate the enhanced flux of cation vacancies, the accumulation of cation vacancies with the acritical concentration occurs at the interface metal/oxide and causes the collapse of the film. The collapse sites in the passive film would make alloy with a dissolution rate when alloy immersed in the chloride containing solution.

In the solution containing both $S_2O_3^{2-}$ and Cl^- ions (NC-2 solution), chloride is strongly absorbed into the alloy surface, and causes a collapse of the film, which promotes the possibility of thiosulfate reacting with metal. The absorbed $S_2O_3^{2-}$ with fully ionized state could reacted with the alloy elements and enhanced the dissolution of alloy 800 because of its structure A () and conjugated structure B (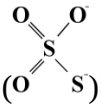)[24]. The possible reactions between thiosulfate and alloy elements are as followed:

$$4M + nS_2O_3^{2-} + 6nH^+ \rightarrow M^{n+} + 2nS + 3H_2O \quad (1)$$

$$8M + nS_2O_3^{2-} + 6nH^+ \rightarrow 2M_2S_n + 4M^{n+} + 3nH_2O \quad (2)$$

Where M means Cr, Fe, Ni, or other metal elements in alloy 800. So the combination of $S_2O_3^{2-}$ and chloride in the solution has a synergistic effect on the anodic dissolution of alloy 800, and thus impede the passivation of alloy 800.

5. CONCLUSIONS

(1) The noise resistance, corrosion potential, breakdown potential and passive range of alloy 800 in the solution containing thiosulfate and chloride ions are lower than that in solution containing thiosulfate or chloride ions alone, whereas the steady state current density of alloy 800 in thiosulfate and chloride containing solution is larger than that in solution containing only thiosulfate or chloride ions.

(2) In the solution containing both $S_2O_3^{2-}$ and Cl^- ions, chloride is firstly absorbed into the alloy surface, and caused the collapse of alloy passive film. The thiosulfate ions in solution with fully ionized state could be absorbed on the collapsed film, reacted with the alloy elements, and thus impeded the passivation of alloy 800 and enhanced its dissolution rate.

ACKNOWLEDGEMENTS
This paper is financially supported by National Key Basic Research Program of China (2011CB610505), and Specialized Research Fund for the Doctoral Program of Higher Education (20120032110029).

References

1. T. Nickchi, A. Alfantazi, *Electrochim. Acta*, 58 (2011) 743-749.
2. R.S. Dutta, J. Nucl. Mater., 393 (2009) 343-349.
3. R.S. Dutta, R. Purandare, A. Lobo, S.K. Kulkarni, G.K. Dey, *Corros. Sci.*, 46 (2004) 2937-2953.
4. R.S. Dutta, Jagannath, G.K. Dey, P.K. De, *Corros. Sci.*, 48 (2006) 2711-2726.
5. N.S. McIntyre, R.D. Davidson, T.L. Walzak, A.M. Brennenstuhl, F. Gonzalez, S. Corazza, *Corros. Sci.*, 37 (1995) 1059-1083.
6. W.-T. Tsai, T.-F. Wu, *J. Nucl. Mater.*, 277 (2000) 169-174.
7. S. Roychowdhury, S.K. Ghosal, P.K. De, *J. Mater. Eng. Perform.*, 13 (2004) 575-582.
8. H.M. Ezuber, *Mater. Des.*, 30 (2009) 3420-3427.
9. C. Duret-Thual, D. Costa, W.P. Yang, P. Marcus, *Corros. Sci.*, 39 (1997) 913-933.
10. R.K. Zhu, J.L. Luo, *Electrochem. Commun.*, 12 (2010) 1752-1755.
11. Z. Fang, R.W. Staehle, *Corros.*, 55 (1999) 355-379.
12. M.G. Faichuk, S. Ramamurthy, W.M. Lau, *Corros. Sci.*, 53 (2011) 1383-1393.
13. D. XIA, J. SHI, W. GONG, R. ZHOU, Z. GAO, J. WANG, *Electrochemistry*, 80 (2012) 907-912.
14. E. García-Ochoa, F. Corvo, *Electrochem. Commun.*, 12 (2010) 826-830.
15. D. Xia, S. Song, J. Wang, J. Shi, H. Bi, Z. Gao, *Electrochem. Commun*., 15 (2012) 88-92.
16. H.A.A. Al-Mazeedi, R.A. Cottis, *Electrochim. Acta*, 49 (2004) 2787-2793.
17. J.M. Sanchez-Amaya, R.A. Cottis, F.J. Botana, *Corros. Sci.*, 47 (2005) 3280-3299.
18. J.M. Sánchez-Amaya, M. Bethencourt, L. González-Rovira, F.J. Botana, *Electrochim. Acta*, 52 (2007) 6569-6583.
19. D.G. Li, J.D. Wang, D.R. Chen, *Electrochim. Acta*, 60 (2012) 134-146.
20. D.S. Kong, W.H. Lu, Y.Y. Feng, Z.Y. Yu, J.X. Wu, W.J. Fan, H.Y. Liu, J. *Electrochem. Soc*., 156 (2009) C39-C44.
21. M. Herranen, J.O. Carlsson, *Corros. Sci.*, 43 (2001) 365-379.
22. D.D. Macdonald, *Electrochim. Acta*, 56 (2011) 1761-1772.
23. Z. Szklarska-Smialowska, *Corros. Sci.*, 44 (2002) 1143-1149.
24. K. Miaskiewicz, R. Steudel, *Angew. Chem.*, 31 (1992) 58-59.

© 2013 by ESG (www.electrochemsci.org)